Mechanism of the Oxidation Reaction of Deoxyhemoglobin As Studied by Isolation of the Intermediates Suggests Tertiary Structure Dependent Cooperativity†

Michele Perrella,*,‡ Richard I. Shrager,§ Marilena Ripamonti,‖ Giacomo Manfredi,‖ Robert L. Berger,§ and Luigi Rossi-Bernardi‡

Dipartimento di Scienze e Tecnologie Biomediche, University of Milano, Milano, Italy, National Institutes of Health, Bethesda, Maryland 20892, and Istituto di Tecnologie Biomediche Avanzate, CNR Milano, Italy

Received November 16, 1992; Revised Manuscript Received March 1, 1993

ABSTRACT: The intermediates in the oxidation of deoxyhemoglobin by ferricyanide in 0.1 M KCl, at 20 °C and three pH values, were studied by cryogenic techniques. Data analysis was carried out according to a simple four rate constant model, ignoring the functional heterogeneity of the subunits, to simulate the time courses of the oxidation reaction, as studied by the stopped-flow technique [Antonini et al., (1965) *Biochemistry 4*, 345], which show anticooperativity at neutral pH and cooperativity at alkaline pH. Data analysis according to a 12 rate constant model indicated that the rate of oxidation of the β subunit in the first oxidation reaction was 4 times faster than the rate of oxidation of the α subunit at pH 6.2 and 12 times faster at pH 8.5. The reactions involving the α subunit were noncooperative except for the last oxidation step at acid and neutral pH, but were cooperative at alkaline pH. The reactions involving the β subunit were partly noncooperative and partly anticooperative. These complex mechanistic patterns suggest that a simple two-state model requiring the concerted transition of the tertiary structures of the subunits from the T to the R conformation is not adequate to interpret the oxidation reaction and that tertiary structures contribute, positively and negatively, to cooperativity. A structural hypothesis is suggested to explain the difference in the reactivities of the α and β subunits.

The kinetics of the reactions of the oxidation of deoxyhemoglobin by ferricyanide as studied by the optical stopped-flow method (Antonini et al., 1965) do not correspond to second-order reactions and show a complex dependence on pH. At a pH below 8, the rate slows down, and a pH above 8, it increases as the reaction proceeds. Similarly complex is the ox–redox equilibrium of hemoglobin. The curve of methemoglobin concentration versus ox–redox potential is sigmoidal in shape at equilibrium and yields a value of n_H[1] = 1.2 at pH 6 and n_H = 2.5 at pH 9 (Antonini et al., 1964). These phenomena were interpreted as either due to negative "heme–heme interaction" or due to functional heterogeneity of the α and β subunits at acid pH (Antonini et al., 1965). Later it was suggested that a decrease in the differences between the functional properties of the subunits with increasing pH was the explanation of the pH effects observed under equilibrium and dynamic conditions (Brunori et al., 1968). This interpretation was contradicted by further kinetic studies indicating an apparent similar difference in the electron affinities of the subunits at acid and alkaline pH (MacQuarrie & Gibson, 1971). A large functional difference between the α and β subunits at neutral pH in the course of oxidation of deoxyhemoglobin by ferricytochrome *c* (Tomoda et al., 1980) and of reduction of methemoglobin by ascorbic acid under anaerobic conditions (Tomoda et al., 1978) was directly demonstrated by the isolation by isoelectric focusing of significantly different amounts of the valence hybrids $\alpha_2^+\beta_2$ and $\alpha_2\beta_2^+$.

A large body of experimental evidence indicates that the slight differences that are observed in some functional properties of the isolated subunits are magnified, under certain conditions, within the assembled hemoglobin tetramer, where they may also vary with the ligation state of the molecule and contribute to the cooperative process (Ackers et al., 1992; Ho, 1992).

Information on the nature and concentrations of the intermediates along all possible pathways of the reaction is crucial for interpretation of the complex mechanisms of hemoglobin reactions. Cryogenic techniques are a powerful tool available now for the study of these problems (Perrella & Rossi-Bernardi, 1981, 1993). Such techniques have been applied to the study of reactions between hemoglobin and carbon monoxide at equilibrium and under dynamic conditions (Perrella et al., 1990, 1992) and can be applied as well to the study of the intermediates in the oxidation–reduction reactions of hemoglobin. Figure 1 shows a scheme describing the multiple pathways of reactions from Hb to Hb^+ by means of 12 rate constants in place of the 16 rate constants of the general scheme. Such a constraint is posed by the inability of the cryogenic technique to resolve species 21 and 22.

In this paper, we report on the isolation of the intermediates in the oxidation of Hb by FeCy at 20 °C and three pH values. Under all conditions, a large range in the concentrations of the intermediates in the same oxidation state was found. The analysis of the data according to the scheme of reactions in Figure 1 indicated significant functional heterogeneity of the α and β subunits and complex mechanistic patterns. The α subunits reacted more slowly than the β subunits in the first oxidation step at all pH values. Along the various pathways

† This work was supported by a grant from CNR, Rome.

* Address correspondence to this author at Via Celoria, 2, 20133 Milano, Italy.

‡ University of Milano.

§ National Institutes of Health.

‖ CNR.

[1] Abbreviations: n_H, Hill coefficient; Hb, deoxyhemoglobin; Hb^+, methemoglobin; CN^-Hb^+, cyanomethemoglobin; FeCy, ferricyanide; IHP, inositol hexaphosphate; *k*, intrinsic rate constant, i.e., apparent constant divided by the statistical factor.

0006-2960/93/0432-5233$04.00/0

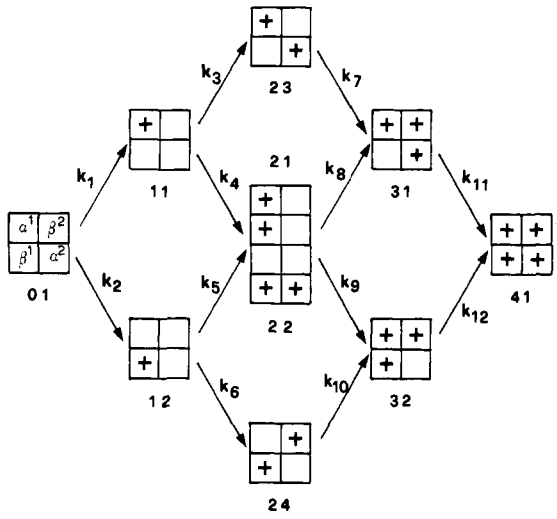

FIGURE 1: Multiple pathways scheme for the reactions of the oxidation of deoxyhemoglobin, species 01, to methemoglobin, species 41. Species 21 and 22 are boxed together, since these species are not resolved by the cryogenic technique.

of reaction in Figure 1, pseudo-non-cooperativity due to the functional difference of the α and β subunits was observed and also cooperativity, noncooperativity, and anticooperativity. We discuss the involvement of the tertiary structure changes in the various observed forms of cooperativity and suggest a structural interpretation of the functional difference between the subunits.

EXPERIMENTAL APPROACH

The techniques and the experimental approach for the isolation of the oxidation intermediates were similar to those used to study the intermediates in the dynamic binding of CO to Hb (Perrella et al., 1992). Briefly, a concentrated solution of Hb was rapidly mixed in a quench-flow apparatus with the solvent containing substoichiometric amounts of FeCy. The oxidation reactions were run to completion (reaction times in the range 100–250 ms) before a sample of solution was quenched into a cryosolvent saturated with CO at −32 °C. The intermediates of the oxidation reactions in the CO-liganded state were then separated by cryofocusing at −25 °C. Since in these experiments the concentrations of the isolated intermediates were not related to the quench time of the reaction, only ratios of the rate constants could be obtained from the analyses of these data according to any selected mechanism. In a few experiments at pH 7 and 8.5, the reactants were quenched before the theoretical amount of Hb^+ was reached. In such cases, the data contained time information and were used to calculate a factor allowing the rate constants to be converted to a real time scale.

METHODS

Preparation of the Reagents. Hemoglobin A_0 was prepared by ion-exchange chromatography from adult blood lysates (Perrella et al., 1992) supplemented with catalase and superoxide dismutase (Boehringer, Mannheim, FRG) to slow down autoxidation reactions, equilibrated with 0.1 M KCl by gel filtration, and stored in liquid nitrogen at a concentration of 12 g/dL. The hemoglobin solution was buffered at pH 7 with 10 mM potassium phosphate and diluted with solvent (0.1 M KCl/10 mM phosphate, pH 7) to 3.7 mM (heme concentration) before deoxygenation in a tonometer. To carry out experiments at pH 6.2 and 8.5, the protein was deoxygenated at neutral pH and then diluted to 3.7 mM concentration with the proper amounts of deoxygenated 0.5 M KH_2PO_4 or 0.5 M Tris in 0.1 M KCl. The Hb^+ content after deoxygenation was 1–2% by the CN^-Hb^+ method (Evelyn & Malloy, 1938).

A 3.7 mM solution of FeCy in 0.1 M KCl, buffered with 10 mM potassium phosphate at pH 6.2 and 7 or with 10 mM Tris at pH 8.5, was diluted with the solvent to yield concentrations of the oxidant corresponding to 15–85% of the hemoglobin concentration value. Deoxygenation of the FeCy solutions was carried out in bottles using pure nitrogen.

Quenching of the Reaction. A description of the quenching technique and of the apparatus is given elsewhere (Perrella et al., 1983, 1992). The reagents were drawn into the syringes of the quench-flow apparatus directly from the tonometer and bottle through Teflon tubings and delivered into a Teflon reaction tube (1-mm inner bore) in a one to one ratio through a ball-mixer (Berger et al., 1968). The reaction times were controlled by adjusting the length of the reaction tube. The reactants delivered to waste through a sampling valve were used to check the pH and hemoglobin concentration. Samples (200 μL) were injected into a vessel thermostated at −32 °C containing 1 mL of 10 mM Tris-HCl buffer in 60% (v/v) ethylene glycol saturated with CO and vigorously stirred. The pH of the hydro-organic buffer at −32 °C was about 10 (Douzou, 1977). Under these conditions, quenching stabilized the hemoglobin tetramers in regard to dimer exchange reactions. When quenching was carried out before the attainment of a Hb^+ concentration equivalent to the FeCy concentration, the binding of CO to the unoxidized subunits and the low temperature of quenching also provided stabilization of the unoxidized subunits against further oxidation. Controls on the effects of the quenching procedure on the various reactions are described elsewhere (Perrella & Rossi-Bernardi, 1993).

Separation of the Intermediates. Cryofocusing on gel tubes of the products of quenching was carried out at −25 °C as previously described (Perrella et al., 1981, 1992). The isolated components were identified and quantitated by chemically assaying the protein eluted from the gel slices containing the components. A detailed description of the procedures and controls is published elsewhere (Perrella & Rossi-Bernardi, 1993). The precision in the determinations of species 11 and, particularly, 23 (see Figure 1) was limited by their paucity and by the partial overlapping of their zones on the gels with the zones corresponding to species 24 and 32, respectively, which were present at greater concentrations. Thus, the precision depended also on the resolving power of the pH gradient, which under constant conditions of solvent and temperature varied slightly with the Ampholine batch (Pharmacia, Sweden) used in the gel preparation.

Data Analysis. To compare the kinetics of the hemoglobin oxidation with the kinetics obtained by the stopped-flow method (Antonini et al., 1965), the following approximate procedure was followed. First, a global fit to the data without time information by Finite Elements (Berger et al., 1993) was carried out to calculate the rate constants for a simple scheme of four consecutive oxidation reactions, assuming $k_4 = 2.5 \times 10^4\ M^{-1}\ s^{-1}$, in the range of values for the apparent second-order rate constant extrapolated to zero time, $O'_{in} = (1.1–4.9) \times 10^4\ M^{-1}\ s^{-1}$, obtained by Antonini et al. (1965). Table I shows the results of these calculations. The time course of the reaction under the conditions of the few experiments at pH 7 and 8.5 containing time information was then simulated using the values of the rate constants in Table I modified by the factor F. This factor was adjusted by trial and error until

Table I: Rate Constants for a Scheme of Four Consecutive Oxidation Reactions of Hb at 20 °C in 0.1 M KCl Buffered at Different pH Values[a]

pH	k_1	k_2 ($\times 10^{-4}$ M^{-1} s^{-1})	k_3
6.2	3.64 ± 0.75	2.42 ± 0.46	2.48 ± 0.38
7.0	4.37 ± 0.97	3.26 ± 0.54	1.83 ± 0.47
8.5	1.81 ± 0.22	1.32 ± 0.12	1.67 ± 0.10

[a] Rate constants calculated by a global fit of the experimental concentrations of the intermediates using Finite Elements, assuming no subunit heterogeneity and $k_4 = 2.5 \times 10^4$ M^{-1} s^{-1}.

the total fractional value of Hb^+ at a reaction time in the simulation equal to the quench time of the experiment was equal to the fractional value of Hb^+ calculated from the concentrations of the oxidation intermediates. Table II shows details of this procedure applied to the data at pH 8.5. The scaling factors at pH 7 and 8.5 were $F = 0.262$ and 0.364, respectively. Data with time information were not obtained at pH 6.2 because the reaction was too fast to be studied with our quench-flow apparatus.

A different procedure of data analysis, based on the solution of a system of differential equations (Shrager, 1992), was used to fit the experimental data and determine the rate constants for the multiple pathways scheme in Figure 1. Briefly, the differential equations are of the matrix form:

$$dy/dt = axy \quad (1)$$

where t = the time of reaction, x = the FeCy concentration, y = a vector of concentrations of the ij species in Figure 1, and a is a constant matrix related to the apparent second-order rate constants for the reaction. Equation 1 is nonlinear because the terms contain products xy of the dependent variables. By changing the variable of integration from t to u such that $du = x\,dt$, eq 1 becomes

$$dy/du = ay \quad (2)$$

which is not linear in y and can be solved analytically. By an iterative method (Newton–Raphson), values of u are found such that $y(u)$ yields the same fractional values of Hb^+ as are observed in the experiments. These fractional values are used as the independent variable for curve-fitting, so that the computed y's can be compared to the corresponding observed y's. By repeating this comparison, the intrinsic rate constants, k's, can be adjusted to optimize the fit using any adequate curve-fitting program. The k's are determined only relative to one of the k's fixed at some value, e.g., unity, since using the fractional value of Hb^+ as the independent variable ignores all information about the time scales of the experiments. In the analyses of our data, we chose the weight to each point as the reciprocal of the sum of a given species, so that the higher the average population of the species, the lower weight it was given. The independent variable was assumed without error. However, since the total fractional value of Hb^+, as calculated from the concentrations of the oxidation intermediates, was a weighted average of eight such concentrations, it probably had less variance than the observed concentrations of the intermediates.

Time information may be recovered using the relation:

$$du = x\,dt \text{ or } dt = du/x(u) \quad (3)$$

From x and $y(u)$, $x(u)$ can be deduced by conservation of matter:

$$x(u) = x - (y_{11} + y_{12}) - 2(y_{23} + y_{24} + y_{21,22}) - 3(y_{31} + y_{32}) - 4y_{41} \quad (4)$$

and the scale factor for the k's then becomes

$$\int_0^{uj} [du/x(u)]/t \quad (5)$$

Multiplying the k's by this factor gives the k's their proper relation to time. Clearly, this procedure could only be applied to the experiments at pH 7 and 8.5 in which the oxidation reaction was not run to completion, i.e., the experiments with time information. The factors at pH 7 and 8.5 were 1.96×10^4 and 1.31×10^4 M^{-1} s^{-1}, respectively.

RESULTS

Simulation of the Kinetics at pH 7 and 8.5. Figure 2 shows simulations by Finite Elements of the reaction kinetics at pH 7 and 8.5 using the rate constants of Table I, converted to a real time scale (see Data Analysis), and the concentrations of the reactants of the stopped-flow experiments of Antonini et al. (1965). Figure 3 shows plots of the apparent second-order rate constant (O') versus the extent of the reaction (% Hb^+) calculated from the simulated kinetics. At pH 7, the apparent second-order rate constant decreased linearly with the extent of the reaction. A deviation from linearity was found at values of % $Hb^+ > 80\%$. The initial and final values of the apparent second-order rate constant obtained by extrapolation of the linear portion of the data in Figure 3 were $O'_{in} = 4.7 \times 10^4$ M^{-1} s^{-1} and $O'_{fin} = 2.1 \times 10^4$ M^{-1} s^{-1}. At pH 8.5, the apparent second-order rate constant increased linearly at values of % $Hb^+ > 40$–50%. Extrapolation of the linear portion yielded $O'_{in} = 1.8 \times 10^4$ M^{-1} s^{-1} and $O'_{fin} = 2.7 \times 10^4$ M^{-1} s^{-1}.

Rate Constants for the Multiple Pathways Scheme. The solution of the linearized system of differential rate equations according to the multiple pathways scheme in Figure 1 yielded the values of the rate constants, relative to $k_2 = 1$, shown in Table III.

Figure 4a,b shows the experimental concentrations of the intermediates at pH 6.2 and 8.5, plotted as fractional values, f_{ij}, versus the total fractional value of Hb^+ and fitted using the rate constants of Table III.

DISCUSSION

Validity of the Experimental Approach. Figure 2 shows that the time courses of the oxidation reactions at pH 7 and 8.5 did not conform to a second-order mechanism. At pH 7, the initial part of the time course indicates an apparent anticooperativity in the reaction. At pH 8.5, the time course indicates an apparent cooperativity, as observed in the stopped-flow kinetics (Antonini et al., 1965). The values of the rate constants obtained by extrapolation of the plots in Figure 3 differ by a factor of 2 from the values reported by Antonini et al. (1965) under similar conditions of temperatures and pH. However, the ratios of the final and initial values are close: $O'_{fin}/O'_{in} = 0.45$, as compared with 0.47 at pH 7 in 0.1 M phosphate, and $O'_{fin}/O'_{in} = 1.5$, as compared with 1.2 at pH 8.5 in 1% borate (Antonini et al., 1965).

The value of the ratio $(O'_{in})_{pH\ 7}/(O'_{in})_{pH\ 8.5} = 2.1$ as obtained by stopped-flow kinetics compares well with the value of 2.6 as obtained from Figure 3, taking into account the approximations involved in the analysis of the data, or with the ratio $(k_1)_{pH\ 7}/(k_1)_{pH\ 8.5} = 2.4$ as calculated from the data in Table I, converted to a real time scale. Thus, we conclude that the optical stopped-flow studies of the oxidation reaction of Hb by ferricyanide and our approach, although methodologically very different, yield qualitatively comparable results.

Multiple Pathways of Reaction. Error Considerations. Owing to the complexity of the multiple pathways scheme in

Table II: Procedure for Calculation of the Scaling Factor (F) Which Converts Rate Constants at pH 8.5 in Table I to a Real Time Scale, Using Data on the Concentrations of Intermediates Containing Time Information (See Experimental Approach) and the Finite Elements Method of Analysis[a]

			($\times 10^{-4}$ M^{-1} s^{-1})								
t (ms)	$[Hb^+]_{obsd}$ (%)	$[Hb^+]_{calcd}$ (%)	k_1	k_2	k_3	k_4	B_0 (%)	B_1 (%)	B_2 (%)	B_3 (%)	B_4 (%)
55	36.9	36.6	0.647	0.472	0.596	0.892	13.0	43.7	29.9	11.0	2.48
							[10.2	45.7	32.1	10.3	1.71]
74	44.2	44.0	0.724	0.528	0.668	1.000	7.5	36.9	33.9	16.6	5.1
							[7.2	34.5	37.5	16.0	5.4]
96	44.8	45.1	0.604	0.440	0.561	0.833	6.7	35.5	34.4	17.6	5.8
							[5.6	37.3	34.8	16.9	5.5]
av k			0.658	0.480	0.608	0.908					
av F = 0.364											

[a] The initial concentrations of the reactants were $[Hb]_0$ = 0.887 mM and $[FeCy]_0$ = 0.556 mM (theoretical total $[Hb^+]$ = 62.7%). The calculated values of the concentrations of the intermediates, B_i (i = 0–4), are compared with the experimental values in brackets.

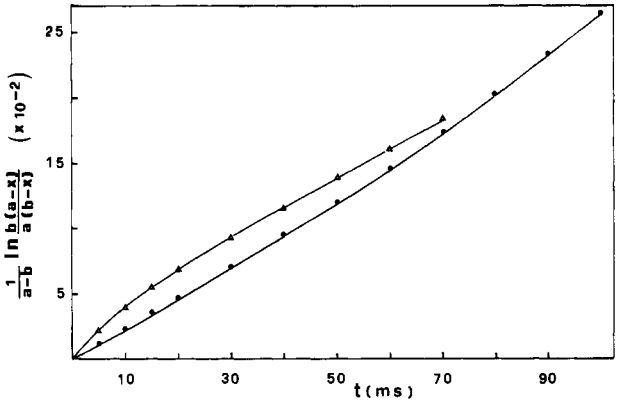

FIGURE 2: Time courses of the reactions at pH 7 (▲) and 8.5 (●) simulated by Finite Elements using the rate constants in Table I converted to a real time scale (see text). a = $[FeCy]_0$ = 1.0 mM; b = $[Hb]_0$ = 0.0175 mM; x = $[Hb^+]$ at time t.

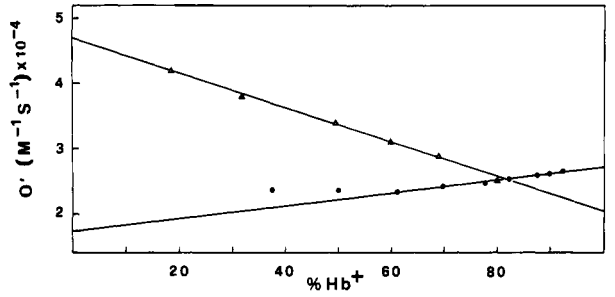

FIGURE 3: Apparent second-order rate constant, O'(M^{-1} s^{-1}), for the oxidation reactions at pH 7 (▲) and 8.5 (●) versus the extent of the reaction, % Hb^+, as calculated from the plots in Figure 2. The extrapolations of the linear portions of the plots yield approximate initial and final values of the constant, O'_{in} and O'_{fin}, respectively (Antonini et al., 1965).

Figure 1, a discussion of the error in the calculated rate constants and of the effects of the accuracy and precision of the data on such calculations can help in assessing the confidence limits of the conclusions we draw in this work.

Extensive controls of the quenching, separation, and quantitation procedures support the accuracy of the determination of the reaction intermediates (Perrella et al., 1992; Perrella & Rossi-Bernardi, 1993). The precision of the quantitation procedure depended on the amount of protein present in the isolated zones. Precision was low (±50–100% error) when the concentrations were ≤1–2% of the total. Thus, the errors in the rate constants along the upper edge of Figure 1, where the species with the lowest concentrations were observed, are larger than the errors in the constants along the lower edge. Moreover, species 11 and 23 partially overlapped

Table III: Rate Constants Calculated from Experimental Values of the Concentrations of Intermediates According to the Reaction Scheme of Figure 1 Assuming k_2 = 1[a]

rate constant	pH 6.2	pH 7.0	pH 8.5
	Oxidation of the α Subunit		
k_1	0.248 ± 0.017	0.178 ± 0.019	0.083 ± 0.010
k_3	0.161 ± 0.027	0.092 ± 0.023	0.272 ± 0.054
k_5	0.260 ± 0.023	0.125 ± 0.020	0.143 ± 0.016
k_8	0.209 ± 0.036	0.113 ± 0.025	0.405 ± 0.060
k_{10}	0.242 ± 0.021	0.113 ± 0.013	0.389 ± 0.027
k_{12}	0.345 ± 0.025	0.258 ± 0.023	0.720 ± 0.038
	Oxidation of the β Subunit		
k_2	1.000	1.000	1.000
k_6	1.076 ± 0.055	1.010 ± 0.057	0.900 ± 0.042
k_4	0.374 ± 0.055	0.485 ± 0.073	0.245 ± 0.087
k_9	0.998 ± 0.089	1.028 ± 0.103	0.764 ± 0.158
k_7	0.033 ± 0.041	0.066 ± 0.066	0.147 ± 0.074
k_{11}	0.509 ± 0.139	0.263 ± 0.132	0.465 ± 0.112

[a] The constants at pH 7 and 8.5 can be converted to real time constants by the factors 1.96 × 10^4 and 1.31 × 10^4 M^{-1} s^{-1}, respectively (see Data Analysis).

on the separation gel with the more abundant species 24 and 32, respectively. As shown in Figure 5, the errors were not normally distributed. However, we estimated that the least-squares approach offered a reasonable statistical approximation. As an alternative to more robust fitting procedures, we tested the effect of the precision in the measurements of the concentrations of species 11 and 23 on the calculated rate constants by making simulations in which the concentrations of these species were increased by various amounts on the assumption of a systematic underestimation. Results are discussed below.

Mechanisms of the Reactions. The reactions in the scheme of Figure 1 can be grouped into three main pathways. The first pathway, referred to in the following as the $\alpha\alpha$-$\beta\beta$ pathway, runs along the upper edge of the scheme. It involves the oxidation of the two α subunits followed by the oxidation of the two β subunits and is centered on species 23. The second pathway, the $\beta\beta$-$\alpha\alpha$ pathway, runs along the lower edge of the scheme. It involves the oxidation of the two β subunits followed by that of the α subunits and is centered on species 24. The third pathway, the α/β pathway, comprising parts of the other two pathways, is centered on the two unresolved species 21 and 22. The four k's of the central part of the α/β pathway, k_4, k_5, k_8, and k_9, are composite constants since the α and β subunits involved in the reactions of species 21 and 22 do not occupy equivalent positions in the two intermediates.

As shown in Table III, in the first oxidation step the rate of oxidation of the α subunit was lower than that of the β

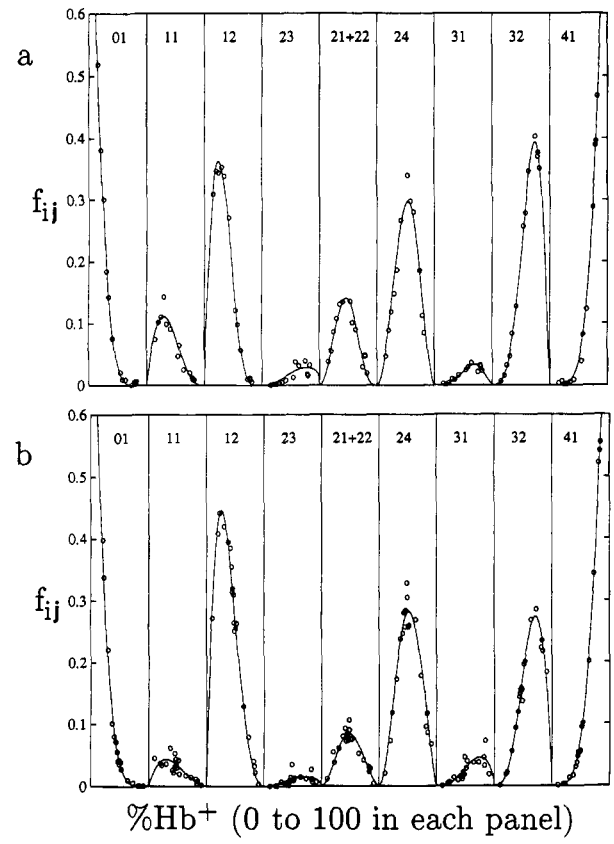

FIGURE 4: Fractional concentrations, f_{ij}, of the oxidation intermediates (Figure 1) versus total fraction of Hb$^+$ (%). (a) Experiments at pH 6.2; (b) experiments at pH 8.5. The lines were calculated using the values of the rate constants in Table III.

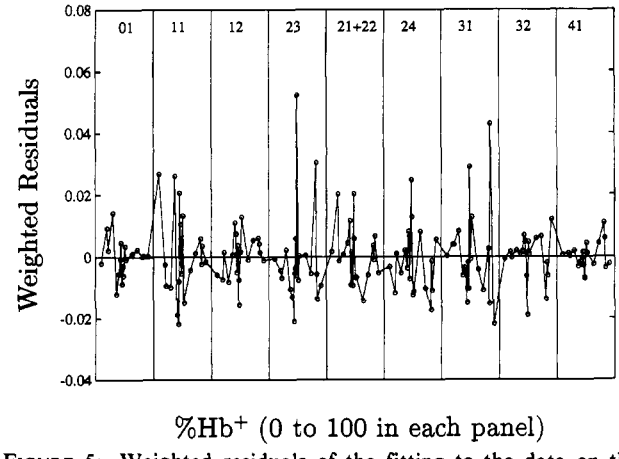

FIGURE 5: Weighted residuals of the fitting to the data on the concentrations of the intermediates at pH 8.5 (panel b in Figure 4) using the rate constants in Table III.

subunit at all pH values ($k_1 < k_2$). Furthermore, the rate of oxidation of the α subunit decreased with increasing pH more than the β subunit (k_2/k_1 = 4 and 12 at pH 6.2 and 8.5, respectively).

At acid and neutral pH, the rate constants for the oxidation of the α subunits along the three pathways were invariant with the exception of k_{12}, which was significantly greater than k_{10}. The rate constant for the oxidation of the β subunits was invariant along the $\beta\beta$-$\alpha\alpha$ pathway ($k_2 = k_6$), but not along the $\alpha\alpha$-$\beta\beta$ pathway ($k_{11} > k_7$) where the rate constant for the oxidation of the first β subunit showed a dramatic decrease with respect to the values observed in the $\beta\beta$-$\alpha\alpha$ pathway ($k_7 \ll k_2$). Thus, along this pathwy, the β subunit appears to "feel" the presence of other oxidized subunits. Since k_4 and k_9 are composite constants, it is not possible to clarify whether such an effect was due to the presence of just one oxidized α subunit on the same dimer or two such subunits, one on each dimer. However, the finding that $k_4 < k_9 \cong k_6$ must imply that species 21 and 22 are functionally nonequivalent.

The low value of k_7 was confirmed by simulations assuming large errors in the concentrations of species 11 and 23 due to their paucity and, in addition, to possible underestimation of their concentrations as discussed above. At pH 7, a 400% increase in the concentration of species 23, and a suitable adjustment in the concentration of 32, yielded a 2–3-fold increase in k_3, while compensatory changes in the values of all the other rate constants were found to be within the range of errors shown in Table III. A 50% increase in the concentrations of species 23 and 11, and suitable adjustments in the concentrations of species 32 and 24, respectively, yielded a dramatic decrease in k_5, while the compensatory changes in the values of the remaining rate constants were again in the error ranges shown in Table III. Both simulations confirmed $k_7 \ll k_2$ and also $k_7 < k_{11} < k_2$.

This study indicates that the apparent anticooperative time course of the oxidation reaction observed by stopped-flow kinetics at acid and neutral pH (Antonini et al., 1965), which was also partly simulated by our data at pH 7, is explained mainly by pseudo-non-cooperativity due to the functional heterogeneity of the α and β subunits in the $\beta\beta$-$\alpha\alpha$ pathway ($k_{10} \ll k_6$) and in the α/β pathway ($k_{12} \ll k_9$). The pseudo-non-cooperativity in the $\alpha\alpha$-$\beta\beta$ pathway ($k_7 < k_3$) contributed less to the overall anticooperative effect, but the low values of k_7 and k_{11} with respect to k_2 and k_6 should have implications on the mechanism of cooperativity and will be commented on later.

At alkaline pH, the rate constants relative to the α subunits indicated cooperativity in all the reactions in which these subunits were involved. The rate constants relative to the reactions of the β subunits along the $\beta\beta$-$\alpha\alpha$ pathway were noncooperative ($k_2 \cong k_6$). Along the $\alpha\alpha$-$\beta\beta$ pathway, k_7 was small compared with k_2 and k_6, although less dramatically than observed at low pH, and again $k_7 < k_{11} < k_2$. The cooperativity in the time course of the oxidation reaction observed by stopped-flow kinetics at alkaline pH is explained, according to our data, by the cooperativity in the processes involving the α subunits and by the reduction in the pseudo-non-cooperativity due to the functional differences between the two subunits. The α and β subunits were still functionally different at pH 8.5, but the values of k_6 and k_{10}, and k_9 and k_{12}, were closer than at neutral or acid pH.

This study indicates that in the oxidation reaction of deoxyhemoglobin the changes in tertiary structure of the subunits contribute to cooperativity and anticooperativity. This is illustrated by the mechanisms of the oxidation of the α subunit at acid and alkaline pH (Table III). At both pH values, the oxidation of Hb to Hb$^+$ brings about a transition in quaternary structure. However, the overall cooperativity brought about by the oxidation of the α subunits was slight at pH 6.2 (k_{12}/k_1 = 1.4) and was determined only by the last oxidation step. At pH 8.5, the overall cooperativity was significantly higher (k_{12}/k_1 = 9), and all the reactions involving the α subunit were cooperative. These data indicate that, regardless of the mechanism yielding the difference in reactivity between the α and β subunits, cooperativity is low under the conditions that favor the T tertiary structure of the α subunit, such as low pH. In fact, according to the stereochemical mechanism of cooperativity described by

Perutz, the salt bridges that stabilize the T structure of the α and β subunits should weaken and eventually break by increasing the pH of the solvent (Perutz, 1970).

A similar destabilizing effect of pH on the β subunits was not observed. This is consistent with the finding that, in the absence of organic phosphate at 0 °C and pH 7.4, 80% of the energy of stabilization of the T structure is localized in the salt bridge formed by the C termini of the β subunits, suggesting that this salt bridge may be more stable than the salt bridge formed by the α subunits under our conditions as well (Ray & Englander, 1986; Louie et al., 1988).

A Working Hypothesis for a Structural Interpretation. The cause of the different reactivities of the two subunits may be a different mechanism of electron transfer from the oxidant to the heme iron or different effects of the tertiary structures of the subunits on such a mechanism. Alternatively, using some of the arguments of the stereochemical mechanism proposed by Perutz for the quaternary structure transition in hemoglobin (Perutz, 1970, 1972, 1989), we suggest that different rates of oxidation, and reduction as well, of the α and β subunits may be determined by different movements of the iron atoms relative to the heme mean plane of the subunits. A shorter movement could imply a slighter change in spin state and slighter perturbations in the tertiary structure in the subunit in the oxidized state with respect to the tertiary structure of the deoxy state and hence a higher rate of oxidation.

The hypothesis is consistent with the crystallographic evidence that in aquomethemoglobin the iron atom of the α subunit, which in deoxyhemoglobin reacts more slowly with ferricyanide, is closer to the heme mean plane than the iron atom of the β subunit, which reacts faster (Ladner et al., 1977).

The rate constants in the reaction of oxidation of deoxyhemoglobin by ferricytochrome *c* are 3 orders of magnitude slower than those in the ferricyanide reaction, suggesting different mechanisms of electron transfer from the oxidants to the heme irons for the two reactions. However, the rate constants along the $\beta\beta$-$\alpha\alpha$ pathway, k' for the oxidation of the β subunits and k'' for the oxidation of the α subunits, yield a value of $k'/k'' = 6$ (Tomoda et al., 1980), remarkably close to the value $k_2/k_{10} = 9$ obtained under similar conditions for the ferricyanide reaction (Table III).

The hypothesis is also consistent with the finding that under anaerobic conditions the β subunits of Hb^+ are reduced by ascorbic acid faster than the α subunits and that IHP causes a 10-fold increase in the rate of reduction of the β subunits (Tomoda et al., 1978). This finding indicates that the rate of the reaction increases under conditions where the reacting subunit is already in a T-like tertiary structure (Tomada et al., 1978; Perutz et al., 1974).

Conclusions. Although our hypothesis is not the only possible explanation for the difference in the rates of oxidation of the α and β subunits of Hb, it is in line with the concept that the spin state of the iron atom, and hence the position of the iron with respect to the heme mean plane, is the major determinant, or trigger as it was named by Perutz, of the changes in tertiary structure of the subunits, which ultimately lead to the change in the quaternary structure of the protein (Perutz, 1989).

In poorly cooperative reactions, such as the oxidation reaction of deoxyhemoglobin reported here, the trigger, according to our hypothesis, is only partially operational, depending on the spin state of the ferric iron, on the type of subunit, and on the conditions, and a large functional heterogeneity of the subunits is observed. In these reactions, tertiary structure changes must contribute, positively and negatively, to the overall cooperativity brought about by the quaternary structure transition.

REFERENCES

Ackers, G. K., Doyle, M. L., Myers, D., & Daugherty, M. A. (1992) *Science 255*, 54–63.

Antonini, E., Wyman, J., Brunori, M., Taylor, J. F., Rossi-Fanelli, A., & Caputo, A. (1964) *J. Biol. Chem. 239*, 907–912.

Antonini, E., Brunori, M., & Wyman, J. (1965) *Biochemistry 4*, 545–551.

Berger, R. L., Balko, B., & Chapman, H. (1968) *Rev. Sci. Instrum. 39*, 493–498.

Berger, R. L., Davids, N., & Perrella, M. (1993) *Methods Enzymol.* (in press).

Brunori, M., Alfsen, A., Saggese, U., Antonini, E., & Wyman, J. (1968) *J. Biol. Chem. 243*, 2950–2954.

Douzou, P. (1977) *Cryobiochemistry*, pp 49–75, Academic Press, London.

Evelyn, K. A., & Malloy, H. T. (1938) *J. Biol. Chem. 126*, 655–662.

Ho, C. (1992) *Adv. Protein Chem. 43*, 154–312.

Ladner, R. C., Heidner, E. J., & Perutz, M. F. (1977) *J. Mol. Biol. 114*, 385–414.

Louie, G., Englander, J. J., & Englander, S. W. (1988) *J. Mol. Biol. 201*, 765–772.

MacQuarry, R. A., & Gibson, Q. H. (1971) *J. Biol. Chem. 246*, 517–522.

Perrella, M., & Rossi-Bernardi, L. (1981) *Methods Enzymol. 76*, 133–143.

Perrella, M., & Rossi-Bernardi, L. (1993) *Methods Enzymol.* (in press).

Perrella, M., Cremonesi, L., Benazzi, L., & Rossi-Bernardi, L. (1981) *J. Biol. Chem. 256*, 11098–11103.

Perrella, M., Benazzi, L., Cremonesi, L., Vesely, S., Viggiano, G., & Berger, R. L. (1983) *J. Biochem. Biophys. Methods 7*, 187–197.

Perrella, M., Colosimo, A., Benazzi, L., Ripamonti, M., & Rossi-Bernardi, L. (1990) *Biophys. Chem. 37*, 211–223.

Perrella, M., Davids, N., & Rossi-Bernardi, L. (1992) *J. Biol. Chem. 267*, 8744–8751.

Perutz, M. F. (1970) *Nature 228*, 726–734.

Perutz, M. F. (1972) *Nature 237*, 495–499.

Perutz, M. F. (1989) *Q. Rev. Biophys. 22*, 139–236.

Perutz, M. F., Heidner, E. J., Ladner, J. E., Beetlestone, J. G., Ho, C. (1974) *Biochemistry 13*, 2187–2200.

Ray, J., & Englander, S. W. (1986) *Biochemistry 25*, 3000–3007.

Shrager, R. I. (1992) *J. Biochem. Biophys. Methods 25*, 113–124.

Tomoda, A., Tsuji, A., Matsukawa, S., Takeshita, M., & Yoneyama, Y. (1978) *J. Biol. Chem. 253*, 7420–7423.

Tomoda, A., Tsuji, A., & Yoneyama, Y. (1980) *J. Biol. Chem. 255*, 7978–7983.